

Photoactivation of pa-GFP in 3D: optical tools for spatial confinement

I. Testa · M. Garrè · D. Parazzoli · S. Barozzi ·
I. Ponzanelli · D. Mazza · M. Faretta · A. Diaspro

Received: 30 September 2007 / Revised: 16 March 2008 / Accepted: 18 March 2008 / Published online: 1 April 2008
© EBSA 2008

Abstract Photoactivatable fluorescent proteins represent an innovative tool for the direct observation of time dependent macromolecular events in living systems. The possibility of switching on a selected and confined subset of the expressed target proteins allows to follow biological processes reaching high signal to noise ratios. In particular, use of non-linear interactions to bring the molecules in the activated fluorescent form make it possible to extend the advantages of photoactivation to events that requires 3D spatial localization. In this work, we show the possibility to realize confined activated volumes in living cells, by employing photoactivatable green fluorescent protein (paGFP) in two-photon microscopy. The analysis of the kinetics of two-photon paGFP activation in dependence of the wavelength, the laser intensity and the exposure time is provided. This study allowed to assess the optimal conditions to induce photoactivation in living samples and to

track the behaviour of tagged histone H2B during cellular division. Furthermore we investigate paGFP photoactivation under evanescent wave illumination. Total internal reflection set-up has been used to selectively activate subresolved distribution of proteins localized in the basal membrane surroundings. These two photoactivation methods provide a suitable tool for many biological applications, combining subresolved surface and in-depth three-dimensionally confined investigations.

Keywords Photoactivatable proteins · GFP · Two-photon excitation microscopy · Total internal reflection microscopy · Fluorescence · Three-dimensional optical microscopy

Introduction

Green fluorescent protein (GFP) from *Aequorea Victoria* (Shimomura 2005) and its multicoloured variations are among the most routinely employed fluorescent tracers in cell biology imaging (Tsien 1998). The need of a more and more precise spatial and temporal localization of proteins and their activity within a cell prompted a new revolution started with Fluorescence Recovery After Photobleaching techniques and prosecuted with the advent of photoactivatable fluorescent proteins (Patterson and Lippincott-Schwarz 2002). Fluorescence of proteins effectively brought a “new light” in molecular and cellular biology studies (Diaspro 2006), opening the way to the ability to monitor molecular dynamics in vivo. The “fluorescence toolbox” is continuously growing (Giepmans et al. 2006), allowing for simultaneous targeting of multiple proteins. Moreover, steps towards macromolecular-scale resolution, using optical microscopes, are becoming reality also thanks to the

Regional Biophysics Conference of the National Biophysical Societies of Austria, Croatia, Hungary, Italy, Serbia, and Slovenia.

I. Testa · D. Mazza · A. Diaspro (✉)
Department of Physics, University of Genoa, 16146 Genoa, Italy
e-mail: diaspro@fisica.unige.it

D. Parazzoli · S. Barozzi · M. Faretta
Department of Experimental Oncology,
European Institute of Oncology, 20141 Milan, Italy

I. Testa · A. Diaspro
LAMBS-MicroScoBio Research Centre,
University of Genoa, 16146 Genoa, Italy

M. Garrè · I. Ponzanelli · A. Diaspro
IFOM, Istituto FIRC di Oncologia Molecolare, 20139 Milan, Italy

A. Diaspro
IBF-CNR, National Research Council, 16149 Genoa, Italy

employment of the photophysical properties of the photoactivation process. Within this pivotal scenario, photoactivatable green fluorescent protein (paGFP) as photoactivatable fluorescent protein, and confocal and two-photon microscopy offered some of the indispensable tools for biological phototracking techniques (Giepmans et al. 2006; Diaspro et al. 2006). Particle tracking inside the cell largely benefits of the ability to spatially and temporally mark specific structures to follow their “signalling” over a “dark” background as made possible since the advent of the pa-GFP. In terms of spatial confinement of the photoactivation process, the use of two-photon or even multiphoton excitation (Schneider et al. 2005) provides several favourable aspects compared to single photon confocal microscopy in photomarking the biological structures to be tracked. The highly confined excitation volumes, of the order of magnitude of subfemtoliter (Diaspro 2001), due to the non-linear requirements provide a unique control of the excitation and consequently photoactivation in the 3D space. Even though single photon confocal laser scanning microscopy can efficiently modulate excitation power in planar sub-micron region, it fails to elicit the same control along the optical axis, being the excitation volume extended to the entire illumination cone of the objective. Beside this aspect, the penetration depth reachable by infrared pulsed lasers can offer unvaluable tools for *in vivo* live cell imaging. The ability to mark specific cells in living embryos by photoactivating biomolecular markers can provide a unique possibility in developmental biology studies to understand cell fate and mechanisms of differentiation. Non-linear spatially controlled protein photoconversion along the optical axis enables to identify single 3D structures and track their spatio-temporal trajectories in a 5D ($x-y-z-t-\lambda$) space. Moreover, the exploitation of non-linear processes involved in the interaction between light and proteins has already led to macromolecular resolution levels keeping the advantages of using optical microscopy (Willig et al. 2006).

In this scenario a deep knowledge of the photophysics of the interaction between light and matter at the basis of the photoconversion process and a characterization of the instrumental parameters able to influence it are strongly desired. Photoactivation efficiency is the result of a competition between photoconversion and photobleaching. Excessive power can paradoxically induce unwanted switching off of the fluorescence. The energy subadministration modalities consequently acquire great importance for the optimization of the process. At the same time the dosage of delivered energy provides a tool for the modulation of the extension of the activated volume, a unique feature of two-photon induced paGFP photoactivation. We present here a characterization in living cells of the relationship between energy flux, varied by irradiation time, and extension of the activated volume. Moreover detailed data on the influence

of the activation time on the efficiency of the activation process were measured. The study on photoactivation by non-linear sources was then completed by showing an *in vivo* biological application for subcellular structures tracking.

Two-photon microscopy is not the only available tool to gain optical confinement of the photoactivation process. Total Internal Reflection Microscopy (TIRF) can be successfully employed to induce paGFP photoconversion of the molecules localized on the basal plasma membrane. We completed the characterization of the kinetics of photoactivation by measuring the relationships between exposure time to an activating evanescent field and efficiency of the photoactivation process.

Materials and methods

Protein immunoprecipitation

Phoenix cells were transfected with PA-GFP encoding DNA using calcium phosphate. After 24 h, cells were lysed in a cold $1\times$ PLC buffer (50 mM HEPES, 1.25% glycerol, 150 mM NaCl, 166 mM $MgCl_2$, 1% TRITON X-100, 0.001% EGTA, 10 mM NaPyruvate, 0.1 mM NaOrtovanadate, 0.01 mM PMSF, aprotinin, pepstatin, and leupeptin) on ice for 1 h. Cell lysates were incubated with an anti GFP polyclonal antibody and subsequently with ProteinA sepharose beads. Proteins immobilized on the surface of the beads were finally cross-linked with 4% paraformaldehyde, in the case of fixed samples. For imaging, beads were resuspended in a 90% glycerol solution.

Cell culture and transfection

U2OS and HeLa cells were grown on coverslips under standard culture conditions at 37°C, 5% CO_2 in a DMEM medium supplemented with 10% North American fetal bovine serum (Gibco Europe, Paisley, UK). The PA-GFP was a generous gift from Dr. George Patterson. Transient transfection was performed using a FuGene (Boehringer-Ingelheim Italia S.p.A., Milan, Italy) reagent according to manufacturer instructions.

Cells were harvested and observed or fixed after 48 h. For TIRF microscopy coverslips were put onto a specific holder and immersed in PBS to maintain the correct refractive index necessary for evanescent field creation.

Total internal reflection fluorescence microscopy

Total internal reflection fluorescence (TIRF) imaging of cells was performed by an Olympus Biosystem TIRF workstation based on Cell[^]R Imaging System (Olympus Biosystems, Munich, Germany). A 405 nm laser diode, 488 nm Ar

laser and 568 nm Kr laser were coupled into an inverted epifluorescence motorized microscope Olympus IX81, and focused at an off-axis position of the objective back focal plane; cells plated on glass coverslips were viewed through an high-aperture 60× objective lens (UIS2 60× TIRFM PlanApo N, NA 1.45, Olympus, Tokyo, Japan) with an additional 1.6× magnification lens. For paGFP imaging a 505 nm dichroic mirror together with a 515–550 nm emission filter was employed. Images (12 bit depth) were acquired using an Orca-ER Cooled CCD digital camera (Hamamatsu Italy, Milan, Italy).

ImageJ image-analysis software (W. Rasband, National Institute of Health, Bethesda, USA) was used for quantitative analysis.

Two-photon excitation microscopy

A Chameleon-XR (Coherent, Santa Clara, CA, USA) Ti:sapphire laser source was directly coupled into the scanning head of a Leica TCS SP2 AOBs confocal microscope using an infrared port. Pulse width lies within the range of 140 fs full-width at half maximum at a repetition frequency of 90 MHz at the laser output window. Measurements were collected using an average power of $\langle P \rangle_{\min} = 1.5$ mW up to $\langle P \rangle_{\max} = 9$ mW at the focal plane for two-photon induced photo-activation. Imaging of the activated protein was obtained using the 488-nm line of a 20-mW Argon ion laser. Images were collected using a 100× oil N.A. = 1.4 objective HCX PL APO (Leica Microsystems S.p.A., Milan, Italy). The two-photon activation process on living cells was first primed by focusing a pulsed infrared laser beam on a region of the sample with $\lambda = 750$ nm¹⁸. Subsequently, the unzoomed area was excited with $\lambda = 488$ nm and $\langle P \rangle = 0.04$ mW (back focal plane of the objective) to follow the activated proteins. The spectral window used for collecting fluorescence was 500–600 nm.

Results

Photoactivation kinetics of paGFP in 2PE-microscopy

paGFP molecules can be efficiently activated under non-linear conditions using infrared laser light in the 720–820 nm wavelength range (Schneider et al. 2005). We used two-photon microscopy to assess in vivo the relationships between activation parameters (i.e. total energy dosage and activating wavelength) and axial confinement of the process. HeLa cells were transfected to express paGFP fused to H2B histone. Parking of the infrared beam was employed to measure the extension of the smallest activatable volume (Fig. 1, Image a). Selected areas, where heterochromatin is accumulated in the cell nucleus, were targeted in order to

work inside spatial regions with negligible concentration gradients consequently avoiding potential artefacts due to inhomogeneous molecular distribution. Monitoring of paGFP-H2B mobility shows that diffusion can be neglected for long time ($t \sim 450$ s, Fig. 2, Graph b) while the fluorescence signal of activated molecules is still visible on a dark background. It was consequently possible to directly measure the extension of the activated volume in living cells without any need of fixation. Measurements were highly facilitated by the dramatic variation in signal to noise ratio obtained after photoactivation. The fold increase of fluorescence in the activated region with respect to the nucleus background fluorescence, due to both auto-fluorescence and non-activated paGFPs fluorescence contribute, reached a factor 60 (Fig. 1, Histogram c). Photoactivation efficiency has been measured as a ratio between fluorescence intensity collected in the activated area before and after exposure to the activating beam, provided that image background was previously subtracted to both the values.

To monitor the relationships between energy dosage and spatial confinement, we activated different points in the cell nucleus by parking the activation laser beam for different irradiation times (1s, 3s) with an average power of 3 mW and a wavelength of $\lambda = 750$ nm. Lateral view of the irradiated nucleus revealed that axial extension of the first activated spot (Fig. 1, Image d, ROI 1) resulted in a confinement of about 1 μm (Fig. 1, Graph e, FWHM). This value is strikingly close to the minimal volume excitable by the non-linear absorption process or equivalently to a measure of the excitation PSF of the two-photon microscope. It is therefore possible to obtain a confinement of the activation process to sub-femtoliter optical volumes. For longer activation time ($t = 3$ s, Fig. 1, Image d, ROI 2) we observed an increased full width at half maximum (~ 1.5 μm) pointing out that the activation confinement strictly relies on the amount of energy delivered to paGFP molecules.

Irradiation power, time and illuminating wavelength are consequently key parameters to localize paGFP photoactivation in space as well as to maximize the obtainable signal to noise ratio. These two requirements are fundamental to achieve a true 3D, even point-like, localization for tracking of molecules in biological systems. In this context, we first examined the two-photon activation efficiency in relation to activation time: variation of the scanning pixel dwell time (activation laser beam permanence on each physical point of the sample) has been employed when irradiating different areas on a paGFP molecular layer to vary the total delivered energy (Fig. 2, Image a: each square was activated with the indicated pixel dwell time value). To avoid artefacts due to inhomogeneity of the sample, sepharose beads (size ~ 80 – 120 μm) with paGFP proteins linked on their surface were employed. Activation has been achieved by zooming in 4.6×4.6 μm regions (pixel size ~ 9 nm)

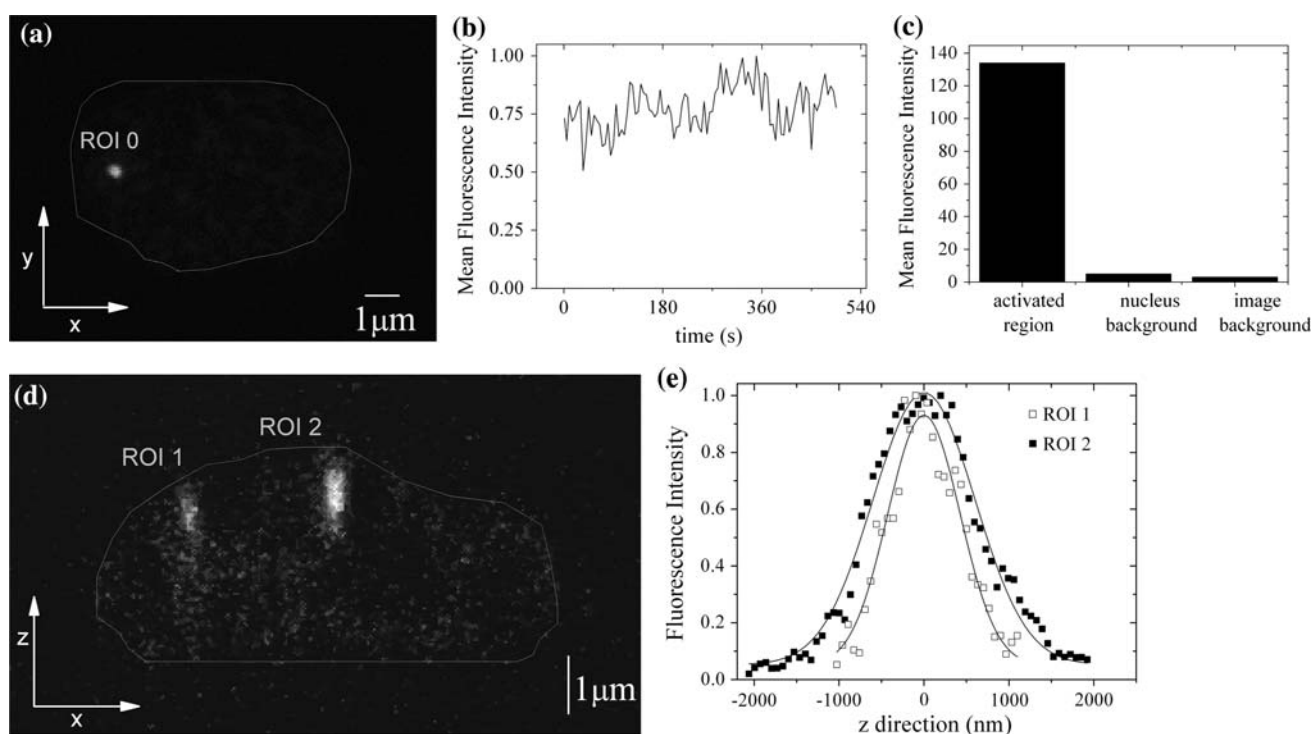


Fig. 1 Two-photon activation 3D confinement in living cells. HeLa cells expressing H2B-paGFP were photoactivated employing a 750 nm wavelength. **a** Photoactivation has been obtained parking the beam on a single point in the field of view for 3 s with an average power of 10 mW. **b** The cell nucleus was subsequently observed for 500 s using $\lambda = 488$ nm and $\langle P \rangle = 0.04$ mW. **c** The histogram shows the mean fluorescence intensity measured: in the activated region after (134 a.u.), and before (5 a.u.) activation together with the image background (3 a.u.). Subtraction of the image background leads to a pre–post-activation

contrast of a factor ~ 66 . **d** A lateral view of the two activated regions in the cell nucleus is shown. The ROIs were obtained parking the beam on a two points for different activation time (ROI 1: 1 s, ROI 2: 3 s) with the same activation power ($P \sim 10$ mW). **e** Intensity profiles of the two ROIs were measured and fitted with a Gaussian function. The Full Width at Half Maximum extrapolated by the fitting curves is, respectively, 1 and 1.5 μm , showing the two-photon activation intrinsic 3D confinement and its dependence on the delivered energy

initially fixing the activation wavelength to 750 nm and employing an average power of 6 mW. Photoproducts have been quantified by monitoring the fluorescence signal increase collected in the post-activation image, obtained exciting the paGFP molecules in the un-zoomed field of view at 488 nm under low power level conditions ($P \sim 0.04$ mW) in order to minimize photobleaching and unwanted activation (Testa et al. 2007).

The same experiment was then repeated by varying the activation wavelength within a range spanning from 720 to 800 nm. Plotting the normalized intensity as a function of time (Fig. 2, Graph b) first revealed an increase in the fluorescence signal due to the growth of the number of activated paGFP molecules and a subsequent decrease caused by photobleaching process predominance. The maximum value of each curve represents the highest contrast between the activated and not activated paGFP protein populations. Activation rate as well as photobleaching kinetics show a clear dependence on the wavelength employed to induce the molecular conversion.

In particular at 720 nm a pixel dwell time of only 4.9 μs allowed to reach the maximal photoactivation

efficiency, while a value of 78.2 μs was required to gain the same effect when a 800 nm wavelength has been employed.

To complete the characterization of the phenomenon, the dependence of photoactivation and photobleaching from irradiation power and duration was measured by fixing the activating wavelength at 750 nm (Fig. 2, Image c).

Each graph reported in Fig. 2 is the result of several independent measurements performed on different beads at four different activation average powers ranging from 1 to 9 mW.

The response, in terms of time required to reach the highest photo-activation efficiency, is strongly influenced by the power employed showing differences of about three order of magnitude for the explored range of activation laser intensity (Table 1). The measured curves rise from the competition of several photo-physical processes varying the number of molecules in the activated state during exposure to the IR light.

For a better comprehension of the fluorescent behaviour detected we developed a simplified model for a preliminary quantitative description of activated protein population

Fig. 2 Power and temporal characterization of two-photon activation process on a gel-beads model system. The contrast reached activating the paGFP molecules shows a strong dependence on irradiation time as exhibited in image (a), where each square region of the beads surface is activated with different irradiation time-intervals at constant activation wavelength (750 nm) and power ($P = 20$ mW). The irradiation time values are shown as pixel dwell time, i.e. the permanence interval of the activation laser light on a single point. Temporal kinetics of two-photon activation process were therefore analysed for different activation wavelengths (b) and four different activation powers 1.5, 3, 6, 9 mW (Graph c, d, e, f). The activations rate K_1 , the photobleaching rate of the activated paGFP form K_2 and the photobleaching rate of the native form K_3 dependence on the activation power is reported in Graph g

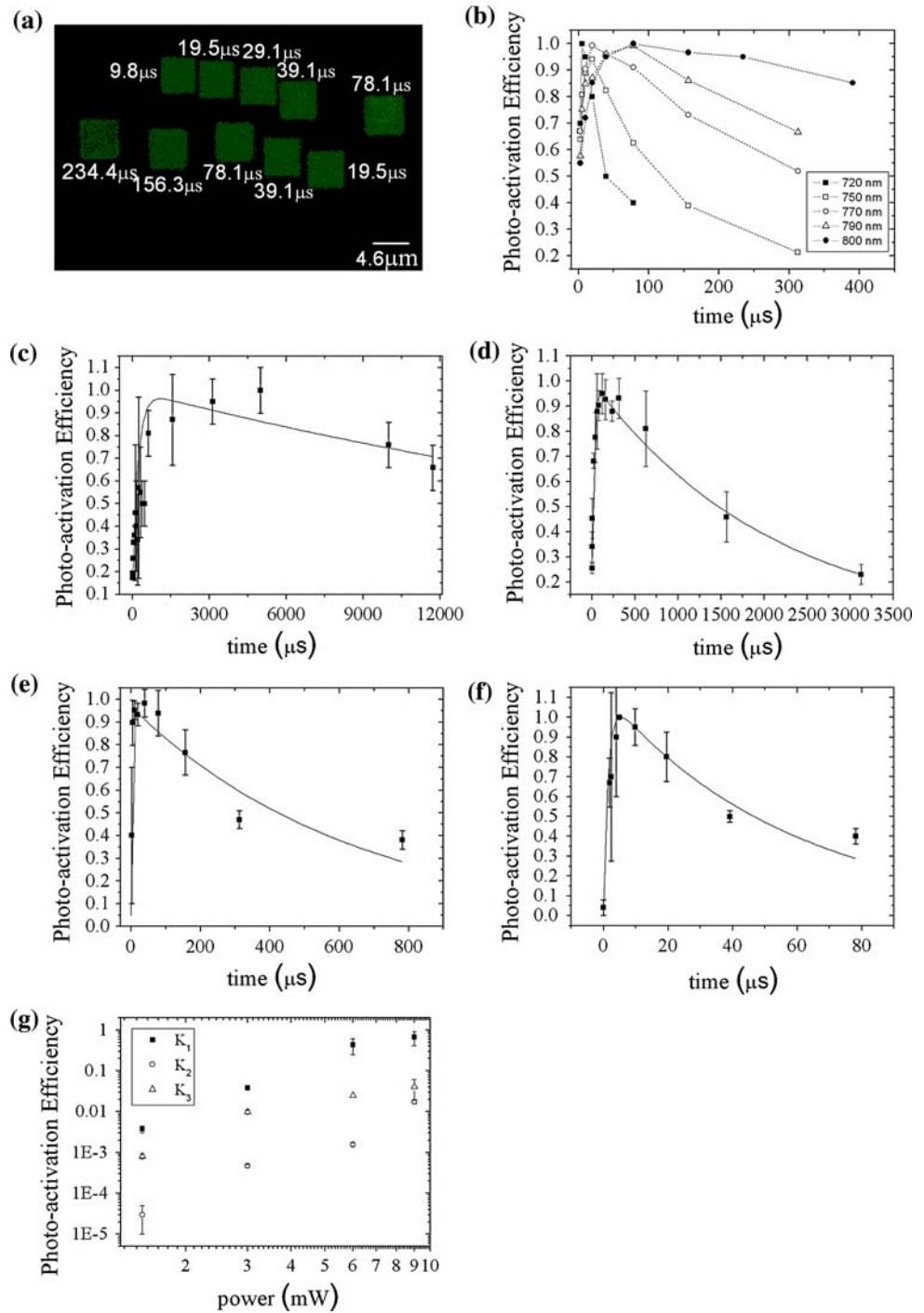


Table 1 Power dependence of the two-photon activation step

Power	1.5 mW (ms)	3 mW (μs)	6 mW (μs)	9 mW (μs)
Irradiation pixel time corresponding to maximum intensity value	(1,562–5,000)	(58–312)	(4.9–78)	(2.4–10)
Photobleaching half time	>12	1,500	300	39.1

We reported the time values related at the maximum intensity collected for each curve obtained at different activation power (within a range of 5–10 mW) and the times relatives to the half-intensity point. These reported values correspond to the pixel dwell time, calculated for a pixel size of 9 nm

kinetics. In particular, we assumed that the main processes involved are the photo-activation of the native paGFP form and the photo-bleaching of both the activated and the native forms. This three state model was employed to fit the curves as shown by the full lines reported on the graphs (c), (d), (e), (f) in order to extrapolate the rates dependence on the power (Fig. 2, Graph g).

The increase of the activation rate K_1 in function of the power lead to an explanation for the shorter time measured to reach the highest activation efficiency while photo-activation resulted to be mainly competed by photo-bleaching of the native paGFP form (K_3). This result is supported by the fact that the wavelength used to induce the photo-conversion of the protein (750 nm) is closer to the two-photon excitation spectrum of the native form (800–850 nm) than the one measured for the activated form (>910 nm). Furthermore, the calculated rates K_1 , K_2 , K_3 , exhibit comparable variations when power was increased thus explaining the invariant activation efficiency reached in different times for the analysed curves.

The obtained results allow for optimization of the photo-activation process both in terms of contrast and confinement in function of the biological event to be tracked and quantified. To show the great potential of the developed protocol we employed non-linear photoactivation to track histones redistribution during cellular division. In particular, a metaphase presenting acrocentric chromosome arrangement was targeted to monitor the DNA partitioning to the daughter cells and observed for the whole mitosis duration (about 45 min). Activation of a confined portion of

the metaphase plate was performed using 750 nm as activation wavelength, a 300 μs pixel dwell time and an average power of 3 mW to avoid cell stress due to irradiation.

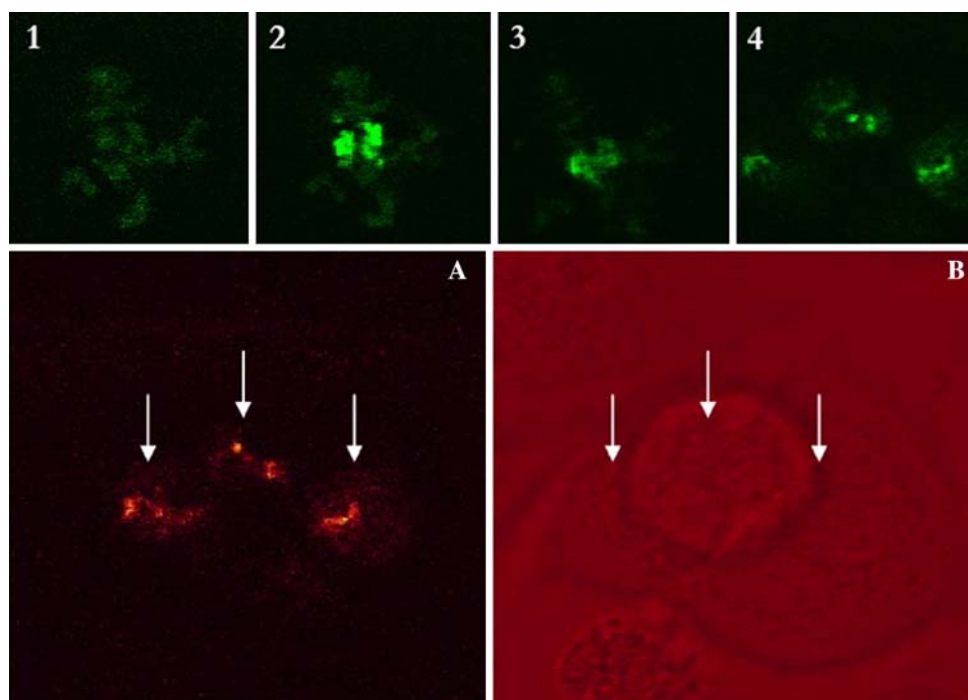
The high signal to noise ratio obtainable in confining photoactivation to the region of interest and the confinement reached by non-linear process allowed to visualize and track the fate of the targeted genomic area upon cell division (Fig. 3). The experimental set-up permits to rapidly switch between two 3D optical techniques: two-photon microscopy to achieve the best confinement of the activation volume and one photon confocal microscopy to observe the movement of the activated paGFPs with maximal spatial resolution.

As shown in the Image 4 of Fig. 3 the activated paGFPs are still visible after 45 min. Furthermore the contrast between the activated and the not activated region is still high enough to recognize the targeted areas in three separate points of the field of view. The comparison of fluorescence and transmission images allows to evidence an almost homogenous distribution of the activated molecules within the body of the three daughters cells (Image a, b of Fig. 3).

Photoactivation kinetics of paGFP in TIRF microscopy

TIRF Microscopy employs the difference in refractive index between the components of the optical system and the sample to create, under critical illumination conditions, an evanescent electromagnetic field. Excitation intensity exponentially decays in 100–200 nm from the interface

Fig. 3 Two-photon activation in living cells: molecular tracking of the nuclear compartment. HeLa cells expressing histone H2B-paGFP were photoactivated with two-photon excitation during mitosis in a region of the metaphase plate. Cell division was sampled at 15-min interval. All images were recorded employing 488 nm excitation. *Point 1* pre-activated signal. *Point 2* localized activation. *Point 3* 30 min after activation. *Point 4* 45 min after activation. Partitioning of the fluorescence signal in three different daughter cells (Image a) evidenced an aberrant division as confirmed by transmitted light morphological examination (Image b)



therefore allowing to image the basal region with an incomparable sectioning ability.

Optimization of a TIRF set up to achieve the best violet transmission allowed to demonstrate the possibility to efficiently employ an evanescent field to confine photoactivation with a very narrow extent along the optical axis (Testa et al. 2008).

To characterize the photoactivation event induced by an evanescent field, a time dependence of the photoconversion has been measured: 405 nm photoactivating pulses of 2 s duration have been alternated by 488 nm TIRF imaging to monitor the increase in the emitted signal. Figure 4 reports a time sequence of photoactivation induced by the violet evanescent field in U2OS cells expressing wild type paGFP. Strikingly a comparison between Widefield and TIRF images reveals that over time the photoactivation of paGFP molecules within the basal layer produced an increase in signal able to mask the fluorescence coming from the not activated inner layers. The two optical schemes becomes therefore equivalent. Widefield microscopy acquires, thanks to the photoconversion process, a sectioning ability comparable to the one provided by TIRF imaging. Mean fluorescence from different cells have been measured and plotted in Fig. 5: an average 2–2.5-fold increase has been reached after 6–10 s of equivalent exposure at 405 nm.

To further investigate the kinetics of the process the effects of continued exposure to the activating field has been evaluated in U2OS cells expressing a paGFP–EGFR fusion protein (Fig. 6). After several activating steps a progressive reduction in the recorded signal has been detected. Kinetics curves from different region of interest inside cells were plotted showing a competition between a photoactivation and a photobleaching effect (Fig. 6a, b) as already

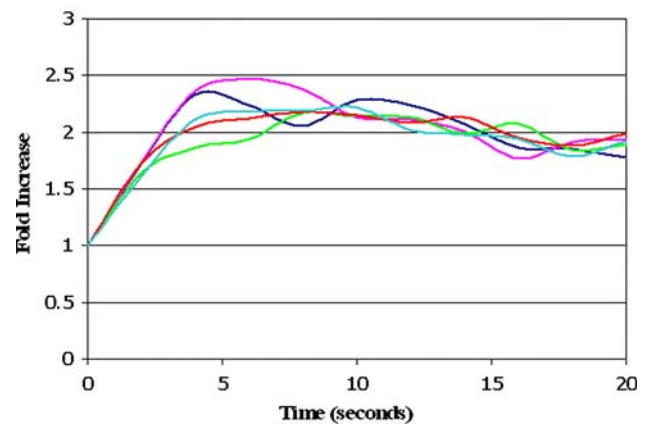


Fig. 5 Dependence of paGFP Photoactivation from the exposure time to the activating evanescent field. The reported graph presents the temporal behaviour of the fluorescence emitted obtained by the experiments described in Fig. 4. Each curve represents the average intensity of basal layers from representative cells

measured in two-photon microscopy. The resulting maximum activation intensity strongly depends on the activation energy rate. The repeated exposure to activating flux can consequently lead to a partial activation of the paGFP molecular native population. If the competing photobleaching process takes place before saturation of the activatable proteins an irreversible decay in the monitored intensity is then observed. The average activation value per cell is consequently the result of a spatially heterogeneous behaviour due to an intensity dependence of both increase and stability of the photo-activated signal. The obtained signal-to-noise increase is in every case lower than the one reached by confocal microscopy supporting the hypothesis that the TIRF activation is not able to extend to the entire molecular

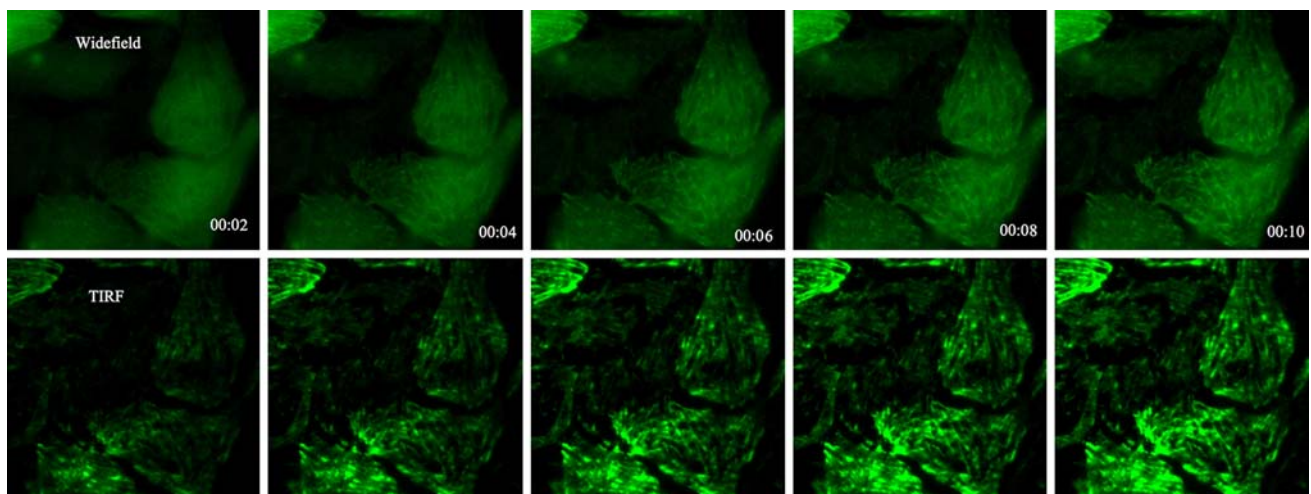


Fig. 4 Dependence of paGFP Photoactivation from the exposure time to the activating evanescent field. U2OS cells were transfected with paGFP to monitor the effect of exposure to increasing energy doses: TIRF Photoactivation was achieved by repeated cycles of stimulation

through a 2 s exposure to 405 nm illumination for activation and subsequent imaging at 488 nm (400 ms camera exposure time) for TIRF imaging and subsequently switching to widefield illumination (470/20 nm excitation filter)

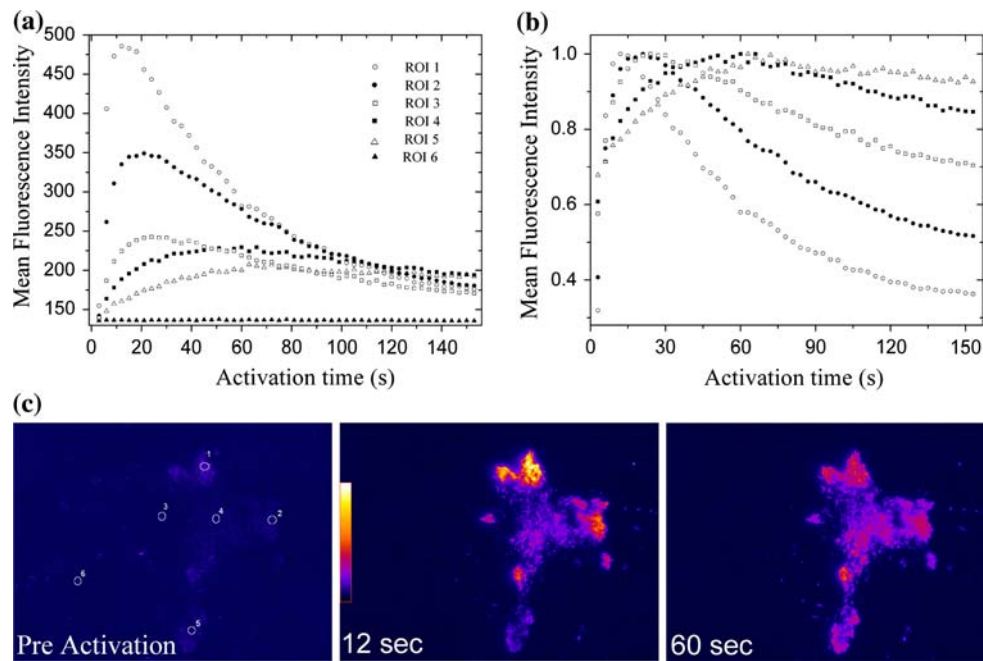


Fig. 6 Kinetics of paGFP-EGFR photoactivation. U2OS cells were transfected with paGFP-EGFR encoding DNA and photoactivated with a 405 nm evanescent field. Repeated cycles of stimulation through a 2 s exposure to 405 nm illumination for activation and subsequent imaging at 488 nm were used to monitor the fluorescence intensity behaviour over time. **a** Temporal evolution of the intensity emitted at 488 nm through selected regions of interest. The most intense regions (ROI 1, 2) show a fast activation associated with a dramatic photodecay. **b** Plot of the intensity versus time curves normalized for the

maximum fluorescence level. A two-step behaviour due to competing effect between photoactivation of the native paGFP molecules and photobleaching of the activated population is evident. **c** Representative images of the temporal kinetics of the activation process. Maximal fluorescence emission was reached at 12 s of equivalent exposure to 405 nm illumination as demonstrated by the sharp increase with respect to the preactivation image. A prolonged illumination beyond the maximal response (60 s) caused a dramatic reduction in the monitored intensity

population. Higher intensity regions presented an increased and faster response that in turn starts to decay once reached the activation peak. Lower intensity regions show a temporal shift to reach maximal photoactivation level but the fluorescence signal is instead conserved over time (Fig. 6a, b).

In TIRF microscopy, a correlation between intensity and distance from the optical interface can be assumed in presence of a homogenous spatial distribution of the receptor on the basal membrane. Lower intensity areas therefore correspond to inner regions receiving a reduced amount of energy less due to the evanescent field exponential decay, thus explaining the retarded effect in both activation and photobleaching. However, the same phenomenon can be ascribed to a concentration dependence effect: high protein levels of expression could determine an increased signal-to-noise ratio enhancing the fold-increase measurement, while a cascade effect in chemical and light induced photobleaching could explain the faster signal decay. An *in vitro* model based on purified protein distribution could provide the basis for the validation of the outlined scenarios enabling to control the concentration variable.

Discussion

The cloning of photoactivatable fluorescence proteins envisaged a revolution in the field of dynamic cellular and molecular imaging. The wide panel of available molecules provided tools not only for studying structure and molecule mobility but also allowed for development of new optical microscopy techniques, such as RESOLFT, breaking the diffraction barrier. However till now a precise characterization of the light-matter interaction leading to the switching on selected photophysical properties and how this is regulated by the experimental parameters of the adopted optical scheme is still lacking.

The normally employed optical tools achieve activation of targeted areas by focused laser beams. Inside this scenario, even in presence of optical sectioning ability, a strong limitation is determined by the loss of confinement of the photoactivation process along the optical axis. Confocal microscopy produces optical slices of finite thickness by filtering out emitted light coming from planes adjacent to the focus position with no limitations on the extent of the illuminated volume along the *z*-axis. Photoactivation, and photobleaching, consequently extend over a volume deter-

mined by the illumination cone of the employed objective. We recently demonstrated that use of alternative microscopies, namely two-photon and TIRF, allow to control the extent of the illumination volume thanks to their intrinsic optical confinement. Energy dosage in two-photon induced photoactivation can be employed to modulate the extension of the z -axis spreading down to the minimal excitable volume determined by the non-linear absorption process in association with the chosen optics. We demonstrated that two-photon illumination allows to target very small regions in living cells without side effects with excellent efficiency in confinement and increase in signal to noise ratio. The spatial control of the photoactivated region opens new perspectives to the analysis of subcellular and molecular motion inside cells. New models to fit the measured data will be consequently required to simulate the new photoactivating geometry. To validate the possibility to perform quantitative imaging, not limited to qualitative observation, we characterized the photokinetics of the process under two-photon excitation. Photoactivation efficiency is essentially a balance between two competing processes, namely photoactivation of native paGFP and photobleaching of activated molecules. We therefore show that, to maintain the possibility to create a quantitative model of molecular dynamics events, attention must be devoted to the optimal combination of activating wavelength, illumination power and duration of the pulse in order to maximize the enrichment of the photoactivated molecular state.

TIRF microscopy bases its ability to confine photoactivation along the optical axis on evanescent fields. We showed that activation can be induced and efficiently confined providing a tool to acquire sectioning ability on the basal layers of the cell even under standard widefield illumination conditions. The energy density involved in a photoactivation process induced by evanescent fields is limited and not able to fully convert the paGFP population present in the illuminated layer. However even under these conditions activation efficiency is again the result of a competition between transitions towards the active state and towards the dark photobleached one. Being the

photobleaching process also mediated by free radicals, darkening can be observed even at these low energies in presence of a large population of activated molecules due to the highly chemically reactive environment created by continuous exposure to the violet activating light. Consequently, even a TIRF optimal set up designed for photoactivation experiments requires careful estimation of the power and duration of the pulse of the activating radiation.

Acknowledgments This work was supported by IFOM (FIRC Institute of Molecular Oncology, Milan, Italy), by Fondazione Compagnia di San Paolo (Turin, Italy), University of Genoa and PRIN2006-MiUR (2006028909) (Ministry of University and Research). The authors are indebted to George Patterson and Jennifer Lippincott-Schwartz for paGFP availability.

References

- Diaspro A (2006) Shine on proteins. *Microsc Res Tech* 69:149–151
- Diaspro A (ed) (2001) *Confocal and two-photon microscopy*. Wiley-Liss, New York
- Diaspro A, Bianchini P, Vicidomini G, Faretta M, Ramoino P, Usai C (2006) Multi-photon excitation microscopy. *Biomed Eng Online* 5:36
- Giepmans BN, Adams SR, Ellisman MH, Tsien RY (2006) The fluorescent toolbox for assessing protein location and function. *Science* 312:217–224
- Schneider M, Barozzi S, Testa I, Faretta M, Diaspro A (2005) Two-photon activation and excitation properties of PA-GFP in the 720–920-nm region. *Biophys J* 89:1346–1352
- Shimomura O (2005) The discovery of aequorin and green fluorescent protein. *J Microscopy* 217:3–15
- Testa I, Mazza D, Barozzi S, Faretta M, Diaspro A (2007) Blue-light (488 nm)-irradiation-induced photoactivation of the photoactivatable green fluorescent protein. *Appl Phys Lett* 91:133902
- Testa I, Parazzoli D, Barozzi S, Garrè M, Faretta M, Diaspro A (2008) Spatial control of paGFP photoactivation in living cells. *J Microscopy* 230:48–60
- Tsien RY (1998) The green fluorescent protein. *Annu Rev Biochem* 67:509–544
- Patterson GH, Lippincott-Schwartz J (2002) A photoactivatable GFP for selective photolabeling of proteins and cells. *Science* 297:1873–1877
- Willig KI, Kellner RR, Medda R, Hein B, Jakobs S, Hell SW (2006) Nanoscale resolution in GFP-based microscopic nature. *Methods* 3:721–723